R477 REVISED NORSOK STANDARD N-004 ON ACCIDENTAL EXPLOSIONS

Abstract

Some of the background for the NORSOK Standard N-004 requirements for design against accidental explosions is presented, including information about ongoing revision of the code. The accuracy of the Biggs' approach (1DOF model) with respect to prediction of maximum displacements is checked by comparison with results of nonlinear finite element analyses. Resistance curve for stiffened plates are compared with results of shell and beam analysis. The ductility limit given in NORSOK is verified, by comparing strains that can be derived from the criterion with strains from finite element shell analysis.

Introduction

The design against explosions is traditionally based upon simplified methods. Notably, has the so-called Biggs' method (Biggs, 1964) become very popular. Biggs' approach is based upon a one degree of freedom (1DOF) idealisation of the fairly complicated non-linear response to an explosion. This facilitates fairly simple estimates to be made of the maximum displacement of a structural component.

Today, the development of computers and algorithms has made possible advanced analysis with the non-linear finite element method (NLFEM) of structural members and subsystems. This eliminates most of the simplifying assumptions that has to be made in the Biggs'- or other methods. However, it is generally not a trivial task to perform non-linear analysis, e.g. the modelling, and execution of the analysis is often demanding with respect to both man-hours and skills.

The simplified methods warrant therefore, still their existence; notably for screening of the severity of the explosion scenarios, reserving NLFEM for the critical cases. Every designer working with NLFEM should have knowledge of the method, allowing him/her to check the validity of the NLFEM results. Consequently, design requirements based on simplified methods remain in many design codes, e.g. both the Interim Guidance Notes (1991) (IGN) and the NORSOK STANDARD N-004 for steel offshore structures subjected to accidental actions (NORSOK 1998).

The purpose of the present work is to present some of the background for the approach adopted in NORSOK. A revision of this code is in the pipeline and the effect of the modifications proposed is particularly studied. It should also be mentioned that Det Norske Veritas is in the process of developing a Recommended Practice (RP) for design against accidental actions (DNV-RP-C204, 2003). This RP will be based upon the revised NORSOK N-004, but will also include a section of design philosophy as well as some very recent achievements. In recognition that it is often challenging to use the proposed method for designers who are not very familiar with the subject, the RP will contain several worked-out examples on the use of the methods to realistic problems in the Commentary sections.

SDOF System Analogy

In his pioneering work Biggs assumed that the structure under action of the dynamic pressure pulse - ultimately attains a deformed configuration comparable to the static deformation pattern. Using the static deformation pattern the dynamic equations of equilibrium can be transformed to an equivalent single degree of freedom system:

$$\left(k_{lm,u}M_u + k_{lm,c}M_c\right)\ddot{y} + K(y)y = F(t)$$

where $k_{lm,u}$ and $k_{lm,c}$ are the load-mass transformation factor for uniform mass, and concentrated mass, $k_{m,u}$ and $k_{m,c}$ are the corresponding mass transformation factors for uniform mass and concentrated mass, k_ℓ is the load transformation factor. M_u and M_c are the total uniform mass and concentrated mass, F is the total load and K is the characteristic stiffness. The advantage with this formulation is that it preserves well known force - stiffness relationships in the linear domain. Characteristic stiffnesses and transformation factors for typical boundary - and load conditions are tabulated in IGN and NORSOK. Factors for beams with two concentrated loads and clamped boundaries have been missing in the current version of NORSOK, but is included in the forthcoming revision.

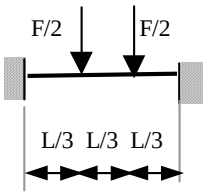

Figure 477.1 New load case for which transformation factors are provided.

The natural period of vibration for the equivalent system in the linear resistance domain is given by

$$T = 2\pi\sqrt{\frac{\bar{m}}{\bar{k}}} = 2\pi\sqrt{\frac{k_{lm,u}M_u + k_{lm,c}M_c}{K_1}}$$

where K_1 is the initial stiffness.

The response, y(t), is - in addition to the load history - entirely governed by the total mass, load-mass factor and the characteristic stiffness.

For a *linear system*, the load mass factor and the characteristic stiffness are constant $K = K_1$. The response is then alternatively governed by the eigenperiod and the characteristic stiffness.
For a *non-linear system*, the load-mass factor and the characteristic stiffness depend on the response (deformations). Non-linear systems are often conveniently be approximated by equivalent bi-linear system. This was introduced by Biggs and is adopted by the IGN and NORSOK. The response can be expressed in terms of:

- K_1 - characteristic stiffness in the initial, linear resistance domain.
- Y_{el} - displacement at the end of the linear resistance domain.
- T - eigenperiod in the initial, linear resistance domain.

For standard load histories and standard resistance curves maximum displacements can be presented in design charts. Often the explosion load is modelled as a triangular pressure with varying rise time and decay times. Assuming that the explosion load can be modelled as a triangular pressure pulse, Biggs presented plots of the maximum displacement of SDOF systems with a bi-linear resistance function. Various curves are presented for various ratios of the limit resistance, R_{el} (corresponding to the formation of a plastic mechanism), and the maximum explosion pressure, F_{max}. When the duration of the pressure pulse relative to the eigenperiod in the initial, linear resistance range is known, the maximum displacement, y_{max}, normalised against y_{el} for a given R_{el}/F_{max} is determined from the diagram as illustrated Figure 477.2.

An extension to the Biggs' method is introduced in NORSOK in the sense that response charts for systems with resistance functions exhibiting strength increase in the large displacement range are provided. This strength increase could be due to membrane action, strain hardening etc., or a combination of these effects. The strength increase is idealised as a third deformation phase with constant stiffness K_3. According to a rigid-plastic approach, the membrane stiffness will be linear, starting from the origin, and this idealisation is therefore used. Charts for three different stiffness are offered, expressed in terms of the initial stiffness, as $K_3 = 0.1K_1$, $K_3 = 0.2K_2$, $K_3 = 0.5K_1$. The response for hardening systems will follow the bi-linear response until the displacement enters the hardening region., as illustrated in Figure 477.2. It is observed that the maximum displacement for such systems ($K_3 > 0$) will be bounded, by contrast to systems with a pure bi-linear resistance. The figure gives also an impression of the accuracy of simplified asymptotic solutions for an impulsive and quasi-static system.

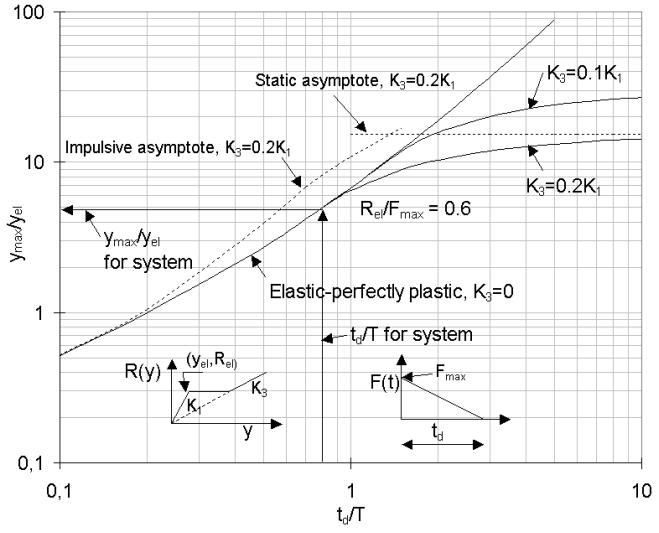

Figure 477.2 Response chart for a 1DOF system with bi-linear and tri-linear resistance function.

Modification for Sheer

The Biggs' method considers members that deform by bending, only. For members with small length to height ratio, shear deformation may become important, notably for members, which can be considered as clamped at the boundaries (e.g. stiffeners subjected to uniform pressure over several frame spacings). In the forthcoming revision of the NORSOK a modification of the resistance function in the linear region and the associated eigenperiod due to shear deformations is proposed.

In the linear phase the stiffness in is modified according to the following formula,

$$\frac{1}{K_1'} = \frac{1}{K_1} + \frac{1}{K_Q}, \qquad K_Q = c_Q \frac{GA_w}{L}$$

where K_1 is the linear bending stiffness, L is the length of the beam, G is the shear modulus and A_w is the shear area.. The shear stiffness depends on the load distribution, with $c_Q = 8$ for uniformly distributed loads, $c_Q = 4$ for one concentrated loads and $c_Q = 6$ for two concentrated loads, independent of the rotational boundary conditions.

The eigenperiod for beams including shear and rotary inertia can be found in many textbooks, e.g. Ron Cook (1983). If both ends are simply supported the following expression is obtained,

$$T = 2\pi \sqrt{\frac{k_{lm,u}M_u + k_{lm,c}M_c}{K_1}} \cdot \sqrt{1 + \left(c_s \frac{\pi r_g}{L}\right)^2 \left(1 + \frac{E}{G}\frac{A}{A_w}\right)}$$

where the boundary condition factor $c_s = 1.0$. M_u and M_c are total distributed mass and concentrated mass, $k_{lm,u}$ and $k_{lm,c}$ are the associated load-mass factors, E is the elastic modulus, A is the total cross-sectional area and r_g is the cross-sectional radius of gyration. The first root term is identical to the conventional formula for the eigenperiod, neglecting shear. The above formula may be used with excellent accuracy with $c_s = 1.5$ for one end clamped and the other end simply supported, and $c_s = 2.0$ for both ends clamped.

Beam Analysis - 1DOF Model vs. NLFEM

The shear effect model outlined above is verified against NLFEM analyses with the space-frame program USFOS (Eberg et. al, 1994) for a beams with different I-cross-sections. The cross-sectional dimensions of the beam, which is 3m long, is shown in Figure 477.3. For simplicity only the height of the profile is changed, keeping the other dimensions constant. The yield stress of the material is $f_y = 300$ MPa.

The effect of shear on the eigenperiod is shown in Figure 477.3. It appears that expression with shear is a very good predictor for the eigenperiod when it is compared with the results of the NLFEM program. It is further noticed that shear has a very moderate influence for a free-free beam, but changes the eigenperiod significantly for L/H<10 in case of clamped-clamped boundaries.

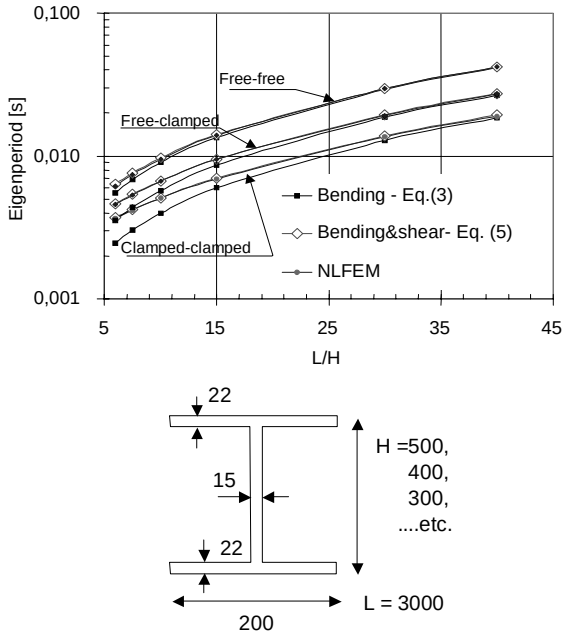

Figure 477.3 Comparison of eigenperiods for I/H-beams calculated with/without the effect of shear and NLFEM.

In order to check the accuracy of the proposed formulations results from 1DOF analysis has been compared with simulations using the nonlinear finite element program USFOS for beams subjected to various triangular pressure pulses with $0.3t_d$ rise times. In order to avoid obscuring the effect of shear flexibility, any effect of shear on the plastic bending moment is not taken into account. The ends of the beam are clamped, but free to move inwards, so no membrane action ("hardening") is generated. The resistance function is therefore considered to be bi-linear. using the so-called equivalent stiffness that preserves the "true" energy dissipation in the resistance up to R_{el}, when a plastic mechanism is formed.

Details of the analyses are given in another paper (J. Amdahl, 2003). The results are summarized in Figure 477.4, which shows the ductility ratios predicted with the 1DOF model compared with NLFEM results. When shear deformation is included, the ductility ratio for the same case is smaller. Generally, there is good agreement between NLFEM and the 1DOF model as concerns the *maximum absolute displacement*. This holds true regardless of whether shear deformations are included or not, for deformation significantly larger than the elastic limit, y_{el}. For small ductility ratios ($\mu < 5$), the shear model is considerably better. The goodness of the pure bending model is somewhat surprising, and leads to the conclusion that the prediction of maximum deformation is relatively insensitive to the stiffness used in the elastic range, so long there is consistence between the elastic stiffness and the associated eigenperiod, and the limit resistance, R_{el}, is correct. The most important effect is, however, that the model including shear predicts the elastic limit (y_{el}) and hence the actual *ductility ratio*, significantly better than the bending model.

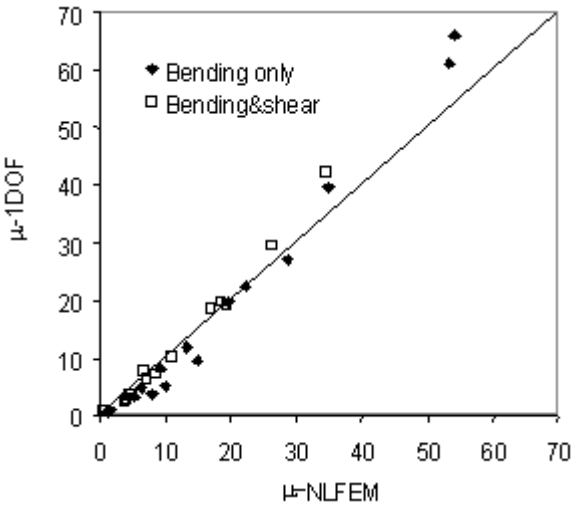

Figure 477.4 Ductility ratios calculated for I- beams with/ without the shear effect compared with NLFEM simulations.

Analysis of Plate-stiffener

In NORSOK stiffened plates are modelled as equivalent beams. The resistance is derived form plastic mechanism theory allowing for membrane stiffening if the ends are fixed or partially fixed against inward displacements. The normalized rigid-plastic resistance curve is shown in Figure 477.5. The plastic collapse resistance in bending for the member

$R_0 = \frac{8c_1 f_y W_P}{\ell}$, where ℓ is member length, f_y is the yield stress, W_P is the plastic section modulus in bending and $c_1 = 2$ for clamped beams and $c_1 = 1$ for pinned beams.

$\overline{w} = \frac{w}{c_1 w_c}$ is a non-dimensional deformation, where

$w_c = \frac{\alpha W_P}{A}$ is the characteristic beam height for beams, with $\alpha =$ 1.2 for stiffened plating. In the elastic range standard beam formulas may be applied.

Relatively small axial displacements have a significant influence on the development of tensile forces in members undergoing large lateral deformations. Curves are therefore given for various degrees of axial restraint, represented by the non-dimensional spring stiffness $c = \frac{4c_1 k w_c^{\,2}}{f_y A \ell}$, where k is the resultant stiffness of the stiffness against pull-in of the member ends and the elastic, axial stiffness of the member.

The accuracy of the 1DOF model has been checked against NLFEM analysis with beam and shell modeling of stiffened plate 1.8 m long and 0.6 m wide and the stiffener is a T-profile with web 180 x 8 mm and top flange 50 x 12 mm. The stiffener is assumed welded to transverse girders, such that the profile shape is preserved at the ends. This is modeled with high stiffness beam elements at the ends of the shell model.

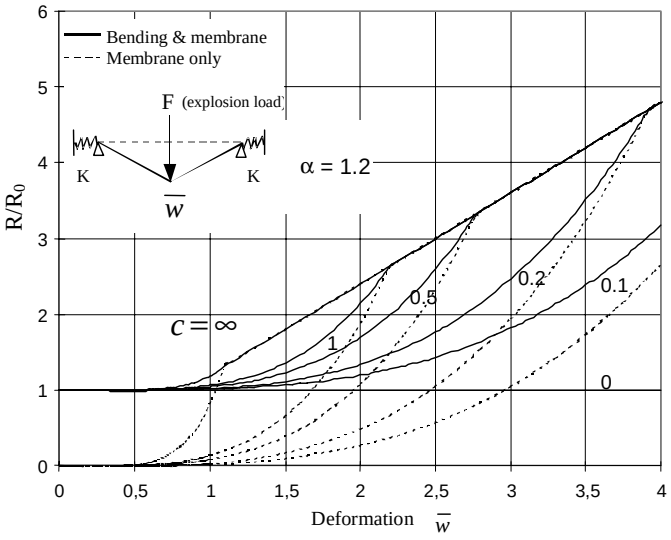

Figure 477.5 Resistance curve for stiffened plates.

It is assumed that the ends are clamped against rotation and either fixed or free axially. Symmetry conditions are imposed on the long edges of the plates. In addition, the edges are assumed to be constrained, i.e. the edges remain straight, but are free to move in. This is ensured by introducing springs with large in-plane shear stiffness on the long edges. The shell finite element model and typical displacement shape at maximum displacement in dynamic analysis are shown in Figure 477.6.

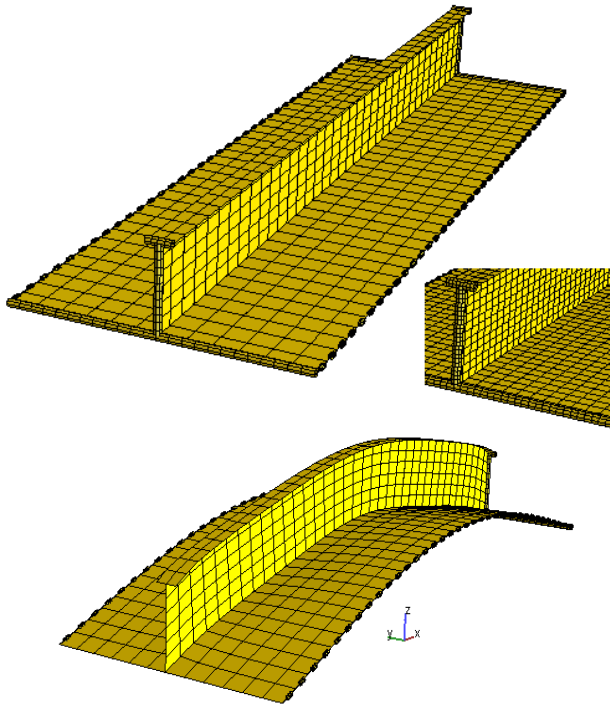

Figure 477.6 Shell element model of plate-stiffener.

The static resistance is plotted in Figure 477.7 (A scale factor of 1.0 corresponds to a uniform pressure of 1.06 MPa). For the shell model plots are provided for both the stiffener at mid-span as well as for the plate midway between stiffeners at midspan. It is observed that the plate deforms significantly relative to the stiffener initially, but as the stiffener collapses, the relative deformation decreases. The resistance predicted by the beam model is somewhat softer than resistance of the shell model using the stiffener displacement, but the agreement is generally quite good. NORSOK resistance curves underestimate clearly the onset of membrane stiffening for axially fixed ends. The reason is that the V-shaped deformation mechanism assumed, does not describe accurately the displacement field for uniformly distributed loads. Fortunately, the use of such resistance functions is conservative; the response to explosion loads will be overestimated. Further comparisons between shell model, beam model and 1DOF models are presented by J. Amdahl (2003).

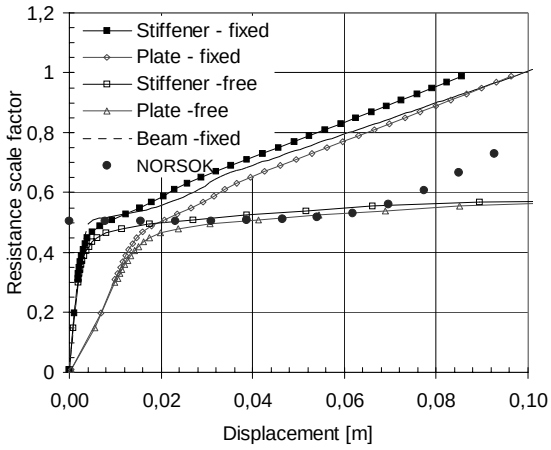

Figure 477.7 Static resistances for stiffened plate.

Ductility limit

A very important issue in conjunction with designing against explosions is the level of deformation that can be assumed prior to rupture of the member. NORSOK offers a ductility limit that is intended for application on resistance curves derived from NLFEM or simple plastic methods based on the plastic hinge concept. The criterion relates lateral displacement at mid-span to the maximum allowable strain. It is derived by integrating the curvatures in the non-linear and strain hardening region to obtain the amount of plastic rotation in the hinges and the corresponding mid-span displacement. The effect of plastic elongation for members exhibiting membrane action due to full - or partial axial restraint is also taken into account. For tubular beams the criterion has been verified previously (Skallerud and Amdahl, 2002).

The critical deformation for initiation of rupture is given as;

$$\frac{w}{d_c} = \frac{c_1}{2c_f}\left(\sqrt{1+\frac{4c_w c_f \varepsilon_{cr}}{c_1}} 4c_w c_f \varepsilon_{cr} - 1\right)$$

where the following factors are defined;

Displacement factor -

$$c_w = \frac{1}{c_1}\left(c_{lp}\left(1-\frac{1}{3}c_{lp}\right)+4\left(1-\frac{W}{W_P}\right)\frac{\varepsilon_y}{\varepsilon_{cr}}\right)\left(\frac{\kappa\ell}{D}\right)^2$$

plastic zone length factor -

$$c_{lp} = \frac{\left(\frac{\varepsilon_{cr}}{\varepsilon_y}-1\right)\frac{W}{W_P}H}{\left(\frac{\varepsilon_{cr}}{\varepsilon_y}-1\right)\frac{W}{W_P}H+1}$$

axial flexibility factor -

$$c_f = \left(\frac{\sqrt{c}}{1+\sqrt{c}} \right)^2$$

non-dimensional plastic stiffness -

$$H = \frac{E_p}{E} = \frac{1}{E}\left(\frac{f_{cr} - f_y}{\varepsilon_{cr} - \varepsilon_y} \right)$$

$c_1 = 2$ for clamped ends, $c_1 = 1$ for pinned ends, c = non-dimensional spring stiffness defined in the previous section, $\kappa l \le 0.5l$ the smaller distance from location of collision load to adjacent joint, W= elastic section modulus, W_p = plastic section modulus, ε_{cr}=critical strain for rupture, $\varepsilon_y = \frac{f_y}{E}$ =yield strain, f_y =yield strength, f_{cr} =strength corresponding to ε_{cr}. The characteristic dimension is taken as: d_c = D diameter of tubular beams, $d_c = 2h_w$ twice the web height for stiffened plates, d_c=h height of cross-section for symmetric I-profiles

For small axial restraint ($c < 0.05$) the critical deformation may be taken as

$$\frac{w}{d_c} = c_w \varepsilon_{cr} .$$

For typical steel material grades the following values for the critical strain, ε_{cr}, and hardening parameter, H, are proposed, refer Table 477.1.

Steel grade	ε_{cr}	H
S 235	20 %	0.0022
S 355	15 %	0.0034
S 460	10 %	0.0034

Table 477.1 Proposed values for ε_{cr} and H for different steel grades

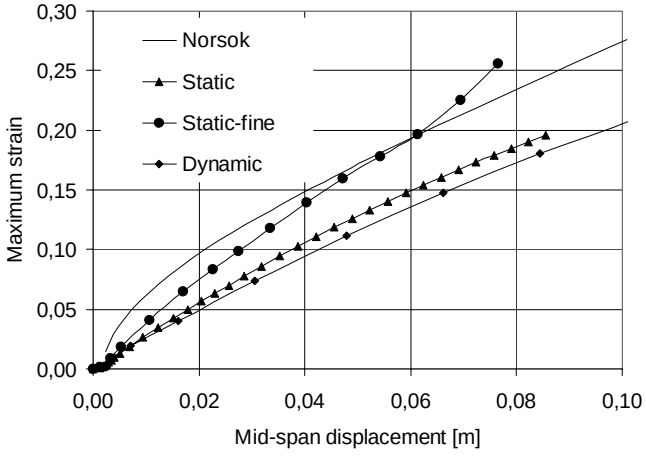

Figure 477.8 Maximum strain versus mid-span displacement for plate-stiffener

If the rupture criterion is inverted, the critical strain may be expressed as a function of the mid-span displacement as shown in Figure 477.8. The figure shows also the maximum strain versus deformation from the finite element simulations of the plate - stiffener. It is observed that the strains from the static shell analyses agree quite well with those obtained in the dynamic analyses, although a small dynamic dependence is evident. A single analysis is performed with the refined mesh indicated in Figure 477.6. While the resistance curves show very little sensitivity to the mesh fineness considered, it appears that the fine mesh yields a noticeable increase in the predicted strain.

The NORSOK ductility relationship performs quite well. Except for the fine mesh at large deformation, the strain that is derived from the criterion is conservative compared to those of the NLFEM simulations, notably for intermediate levels of strain. It should be noticed that elastic displacements are not included in the NORSOK criterion. It is not unreasonable to add the elastic displacement to the value given by the criterion, if the resistance curve includes elastic displacements.

It is a difficult to say what mesh fineness that should be the required. The NORSOK code acknowledges at least the sensitivity of the strain predictions to mesh fineness and specifies that the critical *average membrane* strain for a shell element in NLFEM shell analysis of axially loaded plate material, in lieu of more accurate considerations, should be taken as

$$\varepsilon_{max} = 0.02 + \frac{0.65}{\ell/t} \qquad \ell/t \ge 5$$

where ℓ is the length of element shorter side and t is thickness of plate. In the present case is $\ell/t < 5$ for both meshes, so the same ductility limit will apply.

Conclusions

Comparisons with the results of NLFEM beam analyses show the Biggs' method can provide very satisfactory estimates of the response to accidental explosions, provided that the governing physical effects are represented in the resistance functions. The most important parameter is the limit resistance, corresponding to the formation of a complete mechanism, and correct modelling of the membrane effect, if any.

As concerns prediction of the *maximum absolute deformation*, correct modelling of the stiffness in the linear elastic range is not so important, provided that the ductility ratio μ is large and the calculated eigenperiod corresponds to the stiffness assumed. However, the calculated ductility ratios may be false and criteria for permissible ductility ratios should be used with care.

For short, clamped members shear deformation has a pronounced effect on both the initial stiffness and eigenperiod. It is shown that the formulas, which include the effect of shear, have a very satisfactory predictability for both eigenperiods and maximum deformation. They constitute therefore an improved basis for ductility considerations of short, clamped members.

It is shown that beam modelling of a plate-stiffener performs quite well when compared with results of NLFEM shell analysis. The static resistance of the beam is very similar to the one obtained for the shell, while the simple methods underestimates the resistance and, hence, overestimates the maximum deformation. If the static resistance from NLFEM analysis is used as input to the 1DOF model, Biggs' method works very well.

The resistance the plate-stiffeners studied seem to be invariant with respect to the size of the element mesh actually used. However, for a given case, the strain is clearly mesh size dependent. The NLFEM strains are compared with the strain level that can be derived from the ductility criterion given in NORSOK. It seems that the NORSOK criterion constitutes a reasonable "upper bound" for a plate-stiffener.

References

[1] Amdahl, J. (2003): Design Oriented Methods for Assessment of Accidental Explosion Effects. Response of Structures to Extreme Loading Conference, Toronto 3-6 August, Canada.

[2] Biggs, J. M (1964) Introduction to Structural Dynamics, McGraw Hill, New York.

[3] Craig, R. R. (1981) Structural Dynamic - An Introduction to Computer Methods, J. Wiley & Sons, New York.

[4] Interim Guidance Notes for the Design and Protection of Topsides Structures Against Explosion and Fire, SCI-P-122, The Steel Construction Institute, 1991.

[5] Eberg E., Hellan Ø. and Amdahl, J. (1993): Nonlinear Reassessment of Jacket Structures under Extreme Storm Cyclic Loading- Part III: Development of Structural Models for Cyclic Response, 12th Int. Conf. Offshore mechanics and arctic Eng. , OMAE '93, Glasgow.

[6] NORSOK Standard N-004 (1998) Design of Steel Structures Appendix A Design against Accidental Actions, Norwegian technology Standard Institution, Oslo.

[7] Recommended Practice No. DNV-RP-C204 Design against Accidental Loads, Draft 2002, Det Norske Veritas, Høvik.

[8] Skallerud, B. and Amdahl, J. (2002). Nonlinear Analysis of Offshore Structures. Research Studies Press, Baldoc, Hertfordshire, England

Acknowledgements

The useful discussions and critical comments from Gunnar Solland of Det Norske Veritas to this work are highly appreciated.

Further Information

For further information, please contact:

Jorgen Amdahl
Norwegian University of Science and Technology
NTNU,
7441 Trondheim
Norway

Tel: +47 73 59 55 44
Fax: +47 73 59 55 28
E-mail: jamda@marin.ntnu.no